THE JOURNAL OF PHYSICAL CHEMISTRY B

Article

pubs.acs.org/JPCB

LacI-DNA-IPTG Loops: Equilibria among Conformations by Single-Molecule FRET

Kathy A. Goodson,[†] Zifan Wang,[‡] Aaron R. Haeusler,[†,§] Jason D. Kahn,*[,†] and Douglas S. English*[,‡]

[†]Department of Chemistry and Biochemistry, University of Maryland, College Park, Maryland 20742, United States

[‡]Department of Chemistry, Wichita State University, Wichita, Kansas 67260, United States

Supporting Information

ABSTRACT: The *E. coli* Lac repressor (LacI) tetramer binds simultaneously to a promoter-proximal DNA binding site (operator) and an auxiliary operator, resulting in a DNA loop, which increases repression efficiency. Induction of the *lac* operon by allolactose reduces the affinity of LacI for DNA, but induction does not completely prevent looping in vivo. Our previous work on the conformations of LacI loops used a hyperstable model DNA construct, 9C14, that contains a sequence directed bend flanked by operators. Single-molecule fluorescence resonance energy transfer (SM-FRET) on a dual fluorophore-labeled LacI-9C14 loop showed that it adopts a single, stable, high-FRET V-shaped LacI conformation. Ligand-induced changes in loop geometry can affect loop stability, and the current work assesses loop population distributions for LacI-9C14 complexes containing the synthetic inducer IPTG. SM-FRET confirms that the high-FRET LacI-9C14 loop is only partially destabilized by saturating IPTG. LacI titration experiments and FRET fluctuation analysis suggest that the addition of IPTG induces loop conformational dynamics and re-equilibration between loop population distributions that include a mixture of looped states that do not exhibit high-efficiency FRET. The results show that repression by looping even at saturating IPTG should be considered in models for regulation of the operon. We propose that persistent DNA loops near the operator function biologically to accelerate rerepression upon exhaustion of inducer.

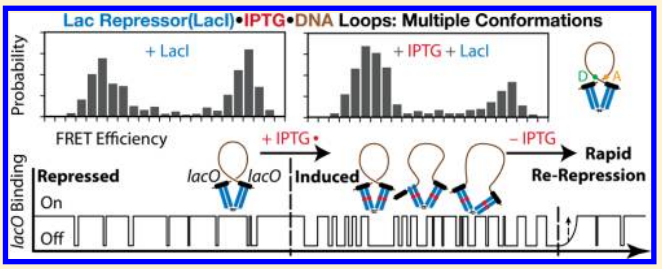

INTRODUCTION

The control of the *lac* operon in *E. coli* by Lac repressor (LacI) is a classic example of negative gene regulation.[1] The LacI homotetramer, a dimer of dimers, has the ability to bind two operator sites simultaneously, forming a DNA loop.[2,3] In part, the biological function of looping is that binding of one dimer to its operator increases the effective local concentration of the other operator around the other dimer, leading to increased occupancy of the second operator.[4] Characterizing this "hydrogen atom of gene regulation" has been of increasing recent interest because the prevalence of looping in prokaryotes and eukaryotes has been recognized.[5,6]

Probing the role of inducers, anti-inducers, and other allosteric effectors is important in understanding the regulation of protein−DNA looped complex shape and stability.[7] In the presence of the artificial inducer isopropyl-β,D-thiogalactoside (IPTG), there is about a 1000-fold decrease in the affinity of LacI for the operator.[8] One IPTG molecule binds to the core domain of one monomer of LacI with a $K_D \approx 5.0 \times 10^{-6}$ M.[8−10] The reorientation of the core domain increases the distance between DNA binding headpieces in a dimer, destabilizing the strong interactions between the headpiece and the DNA operator.[11,12] von Hippel and coworkers explained derepression as the redistribution of IPTG-bound LacI onto nonspecific DNA.[13]

Early in vivo studies of LacI interaction with the *lac* operators demonstrated a sigmoidal curve for derepression as a function of IPTG concentration. This led to belief in either a cooperative or a two-step mechanism, requiring two molecules of inducer to dissociate LacI from the operator.[14,15] Oehler et al.[16] showed that if IPTG binding decreases DNA binding by one dimer, then the sigmoidal curve can be explained by stabilization of binding to the primary operator via binding of an auxiliary operator through DNA looping.[8] In vivo experiments confirmed incomplete IPTG induction of the operon and demonstrated that the efficiency of induced transcription varies periodically with DNA spacing, diagnostic of loop formation.[7,17] Structurally it has been demonstrated that changes in the monomer−monomer interface of LacI result in increased thermodynamic stability of the protein while decreasing affinity for inducer and operator binding.[18] Studies on heterodimeric LacI in which one monomer has a disrupted IPTG binding pocket led to the explicit formulation of LacI as being in an equilibrium between R and R* conformations, where inducer shifts the equilibrium toward the low-affinity R* form.[19]

Special Issue: Paul F. Barbara Memorial Issue

Received: September 7, 2012
Revised: December 24, 2012

   dx.doi.org/10.1021/jp308930c | J. Phys. Chem. B XXXX, XXX, XXX−XXX

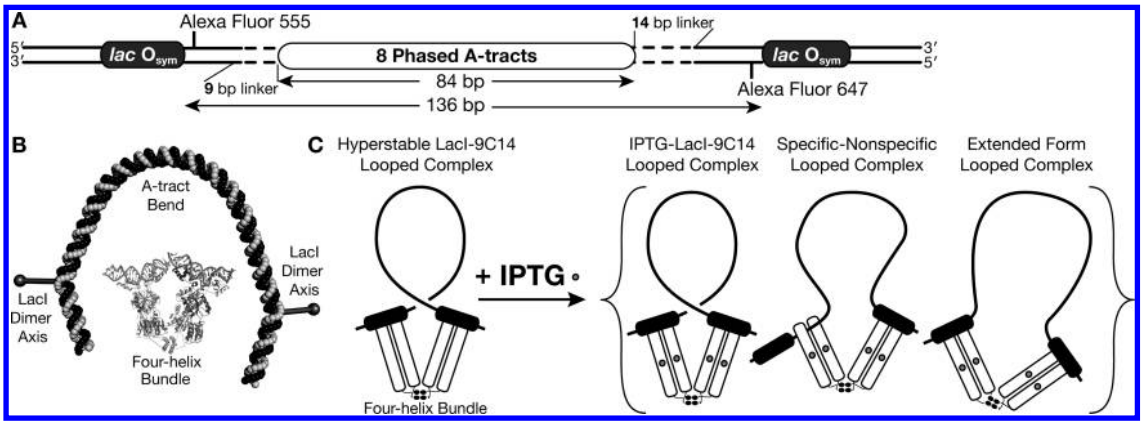

Figure 1. DNA looping construct 9C14 and models for LacI-DNA loops. (A) Schematic of the dual fluorophore 9C14 construct, which is the same as in previous work[28,30,31] except for the use of Alexa Fluor 555 and Alexa Fluor 647 fluorophores. The sequence-induced A-tract bend is flanked by symmetrical operator binding sites. (B) Model for the lowest-energy structure of unbound 9C14 based on the junction model for A-tract DNA bending,[49] assuming a DNA helical repeat of 10.45 bp per turn outside the A tracts. The thick rods indicate the dyad axes of the *lac* operators and hence the LacI dimers within the tetramer. The structure of LacI bound to operator DNA is from PDB file 1LBG,[3] shown approximately to scale. (C) Proposed conversion of the uniform LacI-DNA loop to a set of possible looped complexes upon binding inducer. LacI may change conformation or bind DNA nonspecifically, resulting in the formation of various different loops. Possible single-bound complexes are not shown.

Considering intermediate ligation states, R and R* conformations, DNA binding states including single-bound, double-bound, and loops, multiple loop shapes, and possible nonspecific LacI-DNA interactions there are potentially hundreds of LacI-DNA-IPTG species. Our interests here concern the effects of a bound inducer on DNA site selection and the conformations of DNA loops. Therefore, we carried out our experiments using DNA designed to form exceptionally stable loops, with a protein/DNA ratio of ~1 to further favor looping, and mainly with saturating concentrations of inducer. A complete quantitative understanding of the *lac* operon, and by extension all genes regulated by ligand-responsive DNA looping proteins, will require confronting a more complete structural and thermodynamic characterization of all of the possible protein−DNA−effector complexes.

Loop geometry and stability is modulated by DNA bending strain, protein flexibility, and specific versus nonspecific protein−DNA interactions. In addition, Adhya and coworkers[20] have shown that both parallel and antiparallel trajectories for DNA loops must be considered, and the choice between loop topologies can be dictated by sequence-directed DNA bending.[21,22] Some of the early indications of the importance of DNA bending strain came from the work of the Matthews and Müller-Hill laboratories, where it was shown that LacI binding was stabilized by negative DNA supercoiling.[23,24] Evidence of multiple conformations of the *lac* repressor has been provided by X-ray scattering and electron microscopy, which suggested that LacI could open up from its closed V-shape in solution.[25,26] Tethered particle microscopy (TPM) experiments monitoring the effective length of DNA upon looping by LacI have shown distinct loop states ascribed to multiple conformations of *lac* repressor.[27]

Our introduction of hyperstable LacI-DNA looped complexes whose shape and stability depend on DNA sequence allows the study of alternative loop geometries, DNA binding topologies, and protein conformational changes.[28] The hyperstable DNA constructs contain a sequence directed A-tract bend[29] positioned between two operators (Figure 1). The operator axis dyads are helically phased by changing the length of the two DNA linkers. The two DNA constructs that have been most carefully characterized are denoted 9C14 and 11C12. The dyads face outward for 9C14 and inward for 11C12 relative to the center of curvature of the A-tract bend.[28] The topologies of minicircle products in DNA ring-closure experiments suggested that 9C14 and 11C12 prefer closed-form and open-form LacI-DNA looped complexes, respectively.[22,28] Bulk and single-molecule fluorescence resonance energy transfer (SM-FRET) studies verified that 9C14 does exist in a closed form. Very low FRET efficiencies from 11C12 are consistent with an open LacI-DNA looped complex.[30,31] Evidence from our cyclization,[28] bulk FRET, and SM-FRET experiments lead us to believe that open (and closed) loop forms exist based on opening of the *lac* tetramer. However, subsequent studies from the Perkins laboratory through elastic rod mechanics have shown that our experimental results may be explained with a V-shaped Lac repressor.[21] A subsequent systematic expansion of the bulk FRET/rod mechanics approach confirmed most of the rod mechanics predictions but also supported a role for protein flexibility.[32]

Here we discuss the use of the hyperstable looping constructs to investigate the effects of IPTG on LacI-DNA looped complexes. SM-FRET on freely diffusing LacI-DNA loops allows us to analyze population distributions directly as opposed to the average properties measured in a bulk experiment, and the efficiency of energy transfer should be highly sensitive to changes in loop geometry. The studies presented below confirm that LacI, even at saturating levels of IPTG, forms stable DNA loops. We suggest that the IPTG-bound loops adopt at least two different conformations, one of which is indistinguishable from the loop without IPTG. We speculate that the other form requires either a conformational change in the LacI protein that moves the operators apart or else looping between operator and nonspecific DNA.

MATERIALS AND METHODS

Materials. Restriction enzymes and the Phusion high-fidelity PCR kit were from New England Biolabs and used as directed except as indicated. dNTPs were from USB and [α-^{32}P]dATP was from Perkin-Elmer. Alexa Fluor labeling kits were from Molecular Probes/Invitrogen and were used as directed. DNA oligonucleotides were purchased from IDT. LacI buffer is 25 mM Bis-Tris pH 7.9, 5 mM $MgCl_2$, 100 mM

dx.doi.org/10.1021/jp308930c | J. Phys. Chem. B XXXX, XXX, XXX−XXX

KCl, 2 mM DTT, 0.02% IGEPAL CA-630 (Sigma; replaces nonionic detergent Nonidet P-40), and 50 μg/mL acetylated BSA. IPTG was from Fisher Scientific. The concentration of LacI is expressed as active tetramer throughout, as determined by EMSA titration against excess DNA. LacI protein expression and purification derived from published methods[33,34] as well as the determination of specific activity are described in detail in our recent work[32] and in the Supporting Information.

Synthesis of ^{32}P-Labeled 9C14 DNA. A ~420 bp PCR template was prepared by digesting plasmid pRM9C14[28] with *Bst*NI overnight. The fragment was purified on a 7.5% polyacrylamide (40:1 acrylamide: bis-acrylamide) native gel and stained with ethidium bromide. The DNA template was excised, eluted overnight into 50 mM NaOAc (pH 7.0) and 1 mM EDTA, phenol-chloroform extracted, ethanol precipitated, and stored in TE buffer. The labeled 9C14 DNA looping construct was synthesized using the Phusion high-fidelity PCR system using primers 5′-GCAGGTCAGTCTAGTTAATTGTGAGCGC-3′ and 5′-GCTTTACCACAATGAATTGTGAGCGC-3′, where underlining indicates overlap with the *lac* operator. PCR reactions (50 μL) contained 40 picograms of template, 250 μM of each dNTP, 1 μM of each primer above, 1× Phusion HF reaction buffer, 50 μCi of [α-^{32}P]dATP, and 2 U of Phusion high-fidelity DNA polymerase. PCR cycling conditions were the following: 95 °C for 1 min, 63 °C for 30 s, and 72 °C for 1 min, with the cycle repeated 35 times. The body-labeled PCR product was isolated on an acrylamide gel, and the DNA was extracted from the desired band as above. The purified DNA was resuspended in TE buffer, and the concentrations were calculated based on the incorporation of radiolabel into the final product determined by scintillation counting.

Electrophoretic Mobility Shift Assays in the Presence of IPTG and LacI. Radiolabeled DNA samples (1 nM) were incubated at 21 °C with 0, 0.25, 0.5, 1, 2, and 4 nM LacI in LacI buffer. After 30 min, competitor DNA at 1, 3, and 9 nM was added to the LacI-DNA complex formed at 2 nM LacI. When used, IPTG was at 5 mM. The order of addition for IPTG and LacI had no effects on the results, suggesting that equilibrium was reached. The samples were analyzed on 7.5% polyacrylamide (75:1 acrylamide: bis-acrylamide) gels prepared with and without 5 mM IPTG. The gels and running buffer contained 40 mM tris-borate and 1 mM EDTA, pH 8.3. The gels were prerun for 1 h at 20 V/cm and 21 °C before loading samples. Samples were run for 2 h at 20 V/cm and 21 °C. The gel was dried, exposed to a phosphor screen (16 h), and visualized on a Phosphorimager (Storm 680, Molecular Dynamics).

Fluorescently Labeled 9C14. Fluorescently labeled oligonucleotides 56 nucleotides in length were used as PCR primers for the synthesis of double-labeled 9C14 DNA, which is 216 bp from end to end with internal Alexa Fluor 555 (donor) and Alexa Fluor 647 (acceptor) fluorophores separated by 136 bp. Fluorophores were conjugated to oligonucleotides synthesized with an amino dT C-6 internal modification (T* below: iAmMC6T). Fluorescently labeled oligonucleotides were purified on a 12% polyacrylamide (40:1 acrylamide: bis-acrylamide), 8 M urea gel. The primers were excised, eluted, phenol-chloroform extracted, and ethanol precipitated. The PCR primers are 5′-CTGCAGGTCAGTCTAGGTAATTGTGAGCGCTCACAATTAT*ATCTCAATTCGTACGG-3′ and 5′-CAAGCTTTACCATCAACGAATTGTGAGCGCTCACAATTAT*CTAGCTTCGATTCTAG-3′, with the *lac* operator underlined. Dual fluorophore-labeled DNA constructs were synthesized using the Phusion high-fidelity PCR system with the template described above. PCR reactions (50 μL) contained 40 picograms of template, 200 μM of each dNTP, 1 μM each labeled primer, 1× Phusion HF reaction buffer, and 2 units of Phusion high-fidelity DNA polymerase. PCR cycling conditions were the following: 94.0 °C for 1 min, 55.0 °C for 30 s, 60.0 °C for 30 s, and 72 °C for 1 min for 35 cycles. Purification was carried out as described for the radiolabeled DNA.

Fluorophore Labeling Efficiencies. Labeling efficiencies for Alexa Fluor 555 and Alexa Fluor 647 fluorophore labeled primers were determined by measuring the ratio of dye concentration to DNA concentration using the dye extinction coefficients reported by Invitrogen: $\epsilon^{\text{Alexa555}}$(555 nm) = 150 000 M^{-1} cm^{-1} and $\epsilon^{\text{Alea647}}$(647 nm) = 239 000 M^{-1} cm^{-1}. The dye contribution to absorption at 260 nm was calculated based on their concentrations and their correction factor at 260 nm (CF_{260}). The Alexa Fluor 555 CF_{260} = 0.04, and Alexa Fluor 647 has no contribution at 260 nm. The absorbance of the dye at 260 nm was subtracted, and the concentration of DNA in each sample was then determined using extinction coefficients calculated for single-stranded DNA (33 μg/OD_{260} unit).

Bulk FRET Studies on 9C14. Acceptor- and donor-labeled 9C14 constructs at 2 nM were incubated for 2 min with 0 and 2 nM LacI in LacI buffer. The emission was collected from 550 to 750 nm, with excitation at 514 nm, using a Varian Cary Eclipse fluorescence spectrophotometer with a 10 nm slit width. Following incubation and scanning, 5 mM IPTG was added and allowed to incubate for 2 min, and the emission spectrum was acquired. Additional LacI was added to 8 nM, and the spectrum was acquired again.

SM-FRET Measurements. Single-molecule FRET was done as described previously.[31] Initial LacI titration experiments were used to determine the optimum concentration of LacI to be used. SM-FRET IPTG measurements were conducted at 1 nM 9C14 and 1 to 1.5 nM LacI in LacI buffer. IPTG was added at various concentrations and stages as described in the text. Samples were allowed to equilibrate at room temperature (20 °C) for at least 5 min. Because of the photostability, of the Alexa-labeled DNA, it was not necessary to use an oxygen scavenging or photoprotection system. In addition, we did not observe power-dependence effects previously noted with Cy3-Cy5 that were ascribed to triplet state conversion or blinking.[31]

Single-molecule studies were performed with an oil-immersion objective (Fluar, 100×, N.A. = 1.3, Carl Zeiss, Oberkochen, Germany) inverted microscope with standard methods.[35−37] Excitation at 514 nm was from an argon ion laser focused 10 μm into the sample from the glass−liquid interface. The objective collects the fluorescence burst data as the molecules travel through the beam, and it is then directed through a long pass filter (LP01-514RS, Semrock, Rochester, NY) to remove the excitation wavelength of the laser. The emitted light is subsequently split between two avalanche photodiode single photon counting modules (SPCM-AQR-15, PerkinElmer Optoelectronics, Vaudreuil, Quebec) using a dichroic beam splitter (625DCLP, Chroma, Rockingham, VT). The photon counts are recorded on separate channels of a counter/timer board (PCI 6602, National Instruments, Austin, TX) with 100 μs time bins using Labview 8.5 (National Instruments) software.

SM-FRET Data Analysis. The fluorescence intensities were corrected for background, and bursts that exceeded a threshold total (donor plus acceptor) intensity were selected; the threshold value was chosen in a range where the resulting histogram did not vary significantly with small changes in the threshold and was typically ~30 photons per 100 μs. The apparent FRET efficiency of bursts above the defined threshold is calculated using eq 1:

$$Eff = \frac{I_A}{I_A + I_D} \quad (1)$$

where I_A and I_D are the background-corrected intensities of the acceptor and donor channels. To minimize peak broadening and to retain sensitivity to low-efficiency FRET, we chose not to correct for donor emission that leaks into the acceptor channel, that is, leakthrough correction, which adds to the noise. Without the leakthrough correction, the peak apparent FRET efficiency for the zero ET population is 25%. Leakthrough correction has very little effect on the measured efficiency for the high-efficiency FRET peak. The probability of observing bursts as a function of the apparent FRET efficiency is binned and displayed as in Figures 4 and 5.

To evaluate the effects of added inducer on LacI-DNA loop stability, we conducted a fluctuation analysis using FRET transients acquired with 100 μs time bins in which the instantaneous FRET change, δEff, was calculated from sequential points during prolonged bursts from single LacI-DNA loops:

$$\delta Eff = Eff(t + \Delta t) - Eff(t) \quad (2)$$

where $Eff(t)$ and $Eff(t+\Delta t)$ are two sequential FRET values in a single burst that persisted for greater than 300 μs. The δEff values were sorted according to the value of each $Eff(t)$ and used to construct histograms for high-efficiency ($Eff(t) > 0.5$) and low-efficiency ($Eff(t) < 0.5$) initial observed efficiencies. Figure 6 shows δEff histograms in the presence and absence of IPTG.

RESULTS

Recent in vivo studies have shown that LacI-DNA-IPTG loops are capable of repressing transcription,[7] but they have provided little insight into the geometry of the induced loop. Bulk FRET studies on LacI-induced DNA loops showed that the addition of IPTG resulted in lower observed FRET efficiency, but population distributions could not be obtained.[30] Previous SM-FRET work investigated uninduced loops only and revealed the formation of a closed form loop supporting efficient energy transfer.[31] The analysis of loop population distributions for LacI-DNA-IPTG is the purpose of the current work. We compare the FRET results on loop stability with an electrophoretic mobility shift assay (EMSA). We use bulk and SM-FRET experiments to investigate conformational changes caused by the addition of IPTG to prelooped LacI-induced DNA complexes.

Electrophoretic Mobility Shift Assay Results for LacI-9C14-IPTG Complexes. An EMSA was performed in the absence and presence of inducer (Figure 2). The mobilities of uninduced 9C14-LacI loop, doubly bound $LacI_2$-DNA, and LacI-DNA_2 sandwich mirror those in our previous studies, which identified the bands using titrations of protein and DNA.[28] If we consider the initial formation of a singly bound complex, then the high local concentrations of the remaining

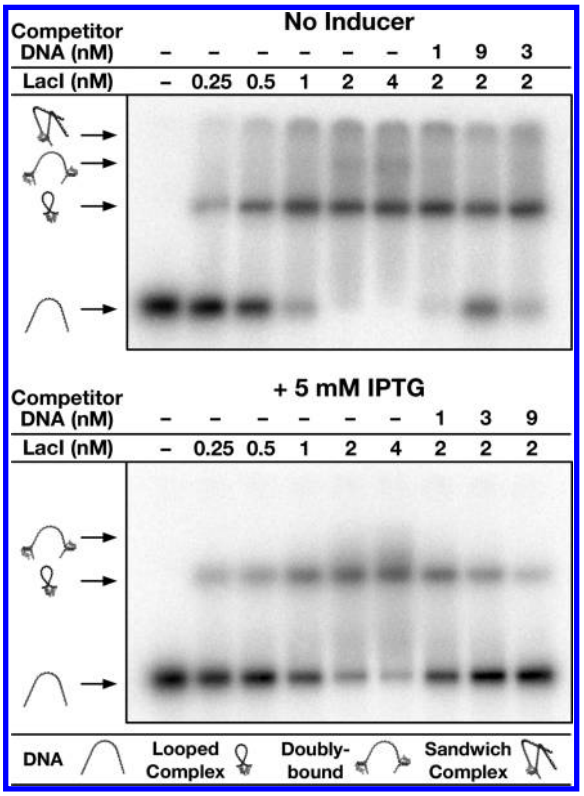

Figure 2. EMSA of IPTG binding to LacI-DNA complexes demonstrates stable LacI-DNA-IPTG loops. Electrophoretic mobility shift studies were performed with 1 nM of ^{32}P-labeled 9C14. The DNA was mixed with 0, 1, 2, and 4 nM of tetrameric LacI for 30 min at room temperature. Following this incubation, 1, 3, or 9 nM of unlabeled 9C14 competitor DNA was added and incubated for an additional 30 min. The upper gel shows controls without IPTG, showing free DNA, a stable looped complex, a smear corresponding to doubly bound DNA that appears at excess LacI, and faint sandwich complexes running near the well that appear with excess DNA. The lower gel, run with 5 mM IPTG in the sample and the gel, shows that the looped complex remains relatively stable but the doubly bound and especially the sandwich complex do not survive electrophoresis.

headpiece of the LacI tetramer and the DNA operator potentiate loop formation. Thus, as expected, the uninduced complex is primarily found as a DNA loop that appears to be a single species. Doubly bound DNA and sandwich complex are formed upon the addition of excess LacI or DNA, respectively. The mobility of our double-bound $LacI_2$-DNA complex is decreased by DNA bending, so it moves more slowly than the looped complex. The sandwich complexes have much lower mobility.

The EMSA in the presence of saturating [IPTG] (5 mM, added to both the binding reaction and the gel) demonstrates that the LacI-DNA looped complex is still formed. The predominant loop does not change in electrophoretic mobility, suggesting that the induced and uninduced loops have similar geometries. The kinetic stability of the induced loop is clearly less than that of the uninduced loop: the addition of competitor DNA to an induced, preincubated complex displaces labeled DNA readily, presumably through a sandwich intermediate. The sandwich and the doubly bound complexes are destabilized by inducer binding or the electrophoresis process, so the loop is the only bound species observed. Free DNA is observed in the presence of IPTG even at increased [LacI], suggesting that a

dx.doi.org/10.1021/jp308930c | J. Phys. Chem. B XXXX, XXX, XXX–XXX

kinetically less stable induced loop breaks down in the gel to some extent.

While the EMSA results demonstrate the existence of a relatively stable LacI-DNA-IPTG loop, the results are not informative as to the loop conformation or solution stability. Caging effects in the gel may alter the stability of the different bound forms and may change the distribution of loop shapes. In contrast, FRET reports on the solution shape, and the remainder of this work applies FRET to the analysis of loop structure and stability in solution.

Bulk FRET Studies. FRET studies on Alexa Fluor 555 and Alexa Fluor 647 fluorophore double-labeled 9C14 DNA with LacI and IPTG (Figure 3) show that addition of saturating inducer to a LacI:DNA loop decreases the sensitized emission of the acceptor to approximately 40% of its original value. DNA labeled with the Alexa dyes behaves similarly to the fluorescein/TAMRA and Cy3/Cy5 pairs used in previous bulk[30] and single-molecule FRET.[31] Control experiments (not shown) confirm that maximal sensitized emission of the acceptor observed at approximately equimolar active LacI and DNA (as in Figure 3) and decreases at higher [LacI]. This decrease may be attributed to specific-nonspecific looping or conversion to doubly bound complexes as seen in the EMSA. The decrease in FRET upon IPTG binding indicates that either a new equilibrium among looped and unlooped states is established, or the transfer efficiency of a stable loop is perturbed. Since FRET does not disappear completely, at least a portion of the DNA must still be bound by protein. To test whether any free 9C14 DNA is present, the LacI concentration was quadrupled at saturating IPTG. The additional LacI should rebind and loop any free 9C14, increasing the energy transfer efficiency, but no such effect was observed, suggesting that IPTG had not caused the dissociation of the original LacI-9C14 complexes. Additionally, any single-bound, unlooped, DNA should have been converted to doubly bound upon addition of excess LacI, pulling the equilibrium to unlooped forms and thereby decreasing FRET efficiency; no such decrease was observed. All of these observations suggest that the LacI-9C14-IPTG complex exists as a stable loop, in agreement with the EMSA results that show a loop under these conditions. However, the initial drop in FRET efficiency with IPTG addition suggests that a structural rearrangement does take place that was not apparent in the EMSA. To identify this structural rearrangement, single-molecule FRET studies were pursued.

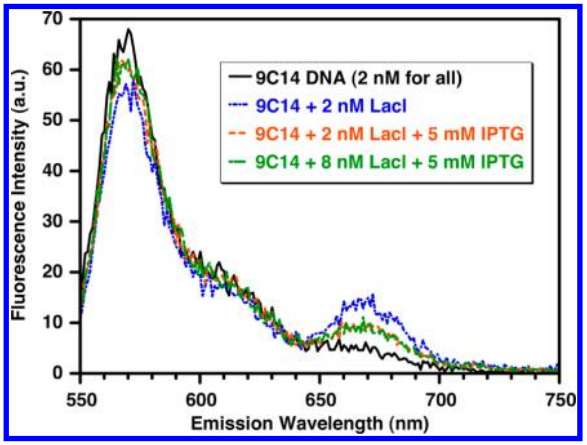

Figure 3. Bulk FRET of LacI-9C14 complexes in the presence and absence of IPTG. Samples were prepared with 2 nM doubly labeled DNA and 0 or 2 nM LacI. After 2 min, IPTG was added to 5 mM final concentration when used, and after a further 2 min, LacI was added to 8 nM to one sample. The sample was excited at 514 nm and the emission spectrum was scanned from 550 to 750 nm. The enhanced emission of the Alexa Fluor 647 acceptor at 670 nm is due to DNA looping. The enhancement is decreased ~2-fold in the presence of IPTG. Excess LacI has no further effect, suggesting that there is no free DNA released during the initial incubation with IPTG. Control experiments (not shown) confirm that 5 mM IPTG is saturating.

Single-molecule LacI-9C14 FRET Results Upon Titration with IPTG. The 9C14 DNA bound to LacI exists substantially in a closed loop form. Based on the interfluorophore distance estimated from the known attachment sites and the LacI-DNA cocrystal structure,[3] the closed loop has an expected FRET efficiency of 0.9.[31] Control histograms (Figures 4A and 5A) show that 9C14 alone exhibits no FRET. Addition of IPTG to the free DNA has no effect on the FRET histogram (not shown). Single-molecule FRET for LacI-9C14 complexes confirms a peak at 90% efficiency (Figure 4). As IPTG is added to the LacI-9C14 loop, the high-efficiency FRET peak decreases in amplitude, but the maximum of the peak does not shift, and significant high-efficiency FRET remains at saturating IPTG concentrations (Panels 4B-4F). After the addition of as little as 0.15 mM IPTG there is no further change at concentrations up to 30 mM IPTG, showing that saturation has been reached. IPTG binding is expected to be less favorable when it is coupled to disruption of a very stable loop, but this effect should simply increase the apparent dissociation constant for IPTG, not prevent IPTG binding, as seen. The persistence of the high-efficiency FRET peak indicates that some of the LacI-DNA-IPTG still exists as a closed form loop, presumably with a geometry similar to the original LacI-9C14 loop.

As the amplitude of the high-FRET peak decreases, the amplitude of the zero-FRET peak increases, but in agreement with the bulk results, the addition of more LacI does not change the zero-peak amplitude further (not shown). This confirms that the molecules that do not exhibit FRET are still looped (because otherwise they would convert to double-bound as above). Other studies on 9C14 suggest that, in fact, some of the molecules that contribute to the zero-FRET peak even in the absence of IPTG are stable loops with alternative topologies.[21,32] The FRET results presented here do not directly bear on the population of zero-FRET loops in the absence of IPTG. The histograms also show bins that depend on LacI and represent intermediate apparent FRET. The fluctuation analysis below suggests that these bins do not reflect possible alternative looped complexes with intermediate FRET efficiencies; rather, the intermediate values are probably due to switching between high- and low-efficiency populations during the time of observation in the beam. Before coming to this conclusion, however, we considered several alternative explanations.

First, a detailed analysis of the photon counting statistics underlying the histograms suggests that the intermediate values are not simply artifacts of counting statistics. Photophysical effects such as acceptor bleaching or blinking also do not explain the results (Supporting Material). The fluorophore labeling efficiencies of these molecules, based on absorbance measurements of primers before PCR, are about 100%. Our other work using the same primers demonstrated that the energy transfer efficiency of 9C14 is not as high as the efficiency of related constructs made from the same primers.[32] These observations confirm that the zero-transfer peak here cannot be

dx.doi.org/10.1021/jp308930c | J. Phys. Chem. B XXXX, XXX, XXX–XXX

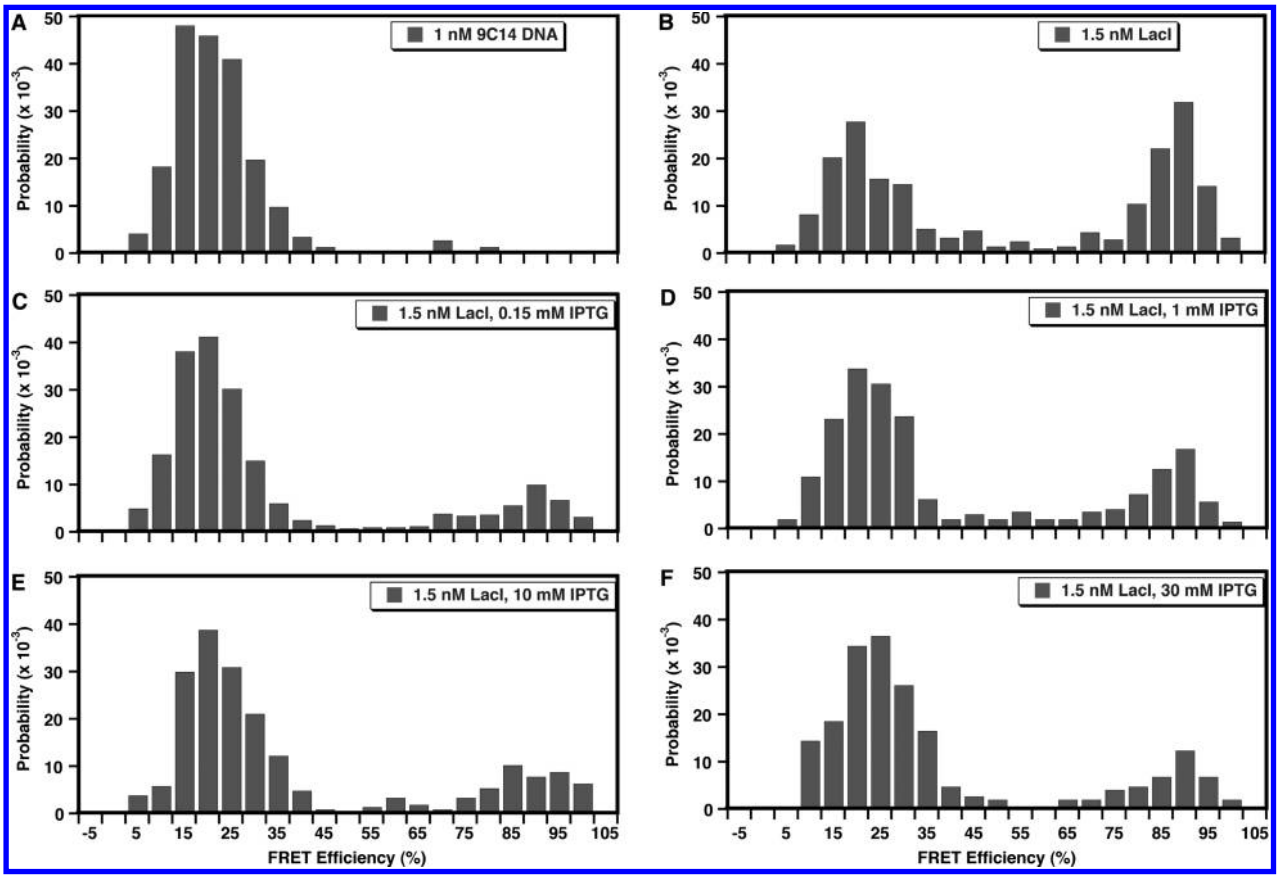

Figure 4. Single-molecule fluorescence experiments on freely diffusing LacI-9C14-IPTG complexes. LacI was incubated with DNA; then, IPTG was added to give the indicated final concentrations. The histograms are normalized distributions of FRET efficiencies calculated from fluorescence collected in donor and acceptor channels upon 514 nm laser excitation of Alexa Fluor 555 and Alexa Fluor 647 dual-labeled samples. (A) Control showing no FRET in freely diffusing 9C14 DNA alone. (B) LacI-9C14 looped complexes show a population with high FRET. (C–F) Histograms obtained from LacI-9C14 complexes with the indicated concentrations of IPTG, ranging from 0.15 to 30 mM. The amplitude of the high-efficiency peak is decreased but not eliminated at saturating IPTG. As discussed in the text, the zero-efficiency peak includes LacI-DNA-IPTG loops that are not FRET active. Conventional error analysis suggests that the intermediate FRET efficiencies seen here and in Figure 5 are not due to intermediate loop populations, as discussed in the main text and in the Supporting Information.

entirely due to molecules with bleached acceptors. This is at odds with our previous single-molecule FRET studies on 9C14;[31] that work used Cy3-Cy5 fluorophores that were subject to blinking,[38] and the data analysis was not as sophisticated as the current work.

Single-Molecule 9C14/LacI FRET Results with LacI Pre-Incubated with IPTG. The loops formed on 9C14 and related molecules are extremely stable to loss of LacI, raising the possibility that the intermediate FRET efficiencies could be due to nonequilibrium loop distributions. To test this idea, we carried out parallel studies in which LacI was mixed with IPTG before the addition of DNA, with the results shown in Figure 5. The same high-FRET and low-FRET peaks are still present at similar amplitudes, confirming that the essential results are independent of the order of addition. However, the intermediate-efficiency apparent FRET values are more prominent in Figure 5. This may be due to more rapid kinetics of interconversion between the loop geometries when LacI is preincubated with IPTG, but more experimentation will be required to test this.

In other experiments similar to those of Figures 4 and 5 (i.e., with or without preincubation with IPTG), histograms obtained at 0.5 μM and 5 μM IPTG are similar to those from the uninduced LacI-9C14 controls (data not shown). Measurements at 50–300 μM IPTG are usually indistinguishable from the results shown in Figures 4 and 5, which are for $\geq$1 mM IPTG. We have occasionally observed distributions with intermediate amplitudes for the high-FRET peak, but given the variation apparent in Figures 4 and 5 these cannot be confidently assigned to actual mixtures of loops with and without IPTG. However, we have never observed a substantial shift in the position of the high-FRET peak. The transition between induced and uninduced loops would be expected to be quite sharp upon binding of inducer due to stabilization of the induced conformation of the repressor.[19] The observed variability in the midpoint concentration of IPTG might also be due to variable adsorption of IPTG in the sample cell.

Fluctuation Analysis of FRET Transients. To investigate the effects of IPTG on the kinetic stability of looped conformations and to evaluate whether interconversion between the equilibrium loop geometries can be observed, we extracted the amplitudes and signs of rapid fluctuations in FRET efficiency in 9C14-LacI loops using data obtained with 100 μs acquisition times. The fluctuations δEff originating from low- and high-efficiency FRET states were evaluated separately. Fluctuation histograms in the presence and absence of IPTG are shown in Figure 6. The results are interpreted in terms of a pseudo-two-state equilibrium:

dx.doi.org/10.1021/jp308930c | J. Phys. Chem. B XXXX, XXX, XXX–XXX

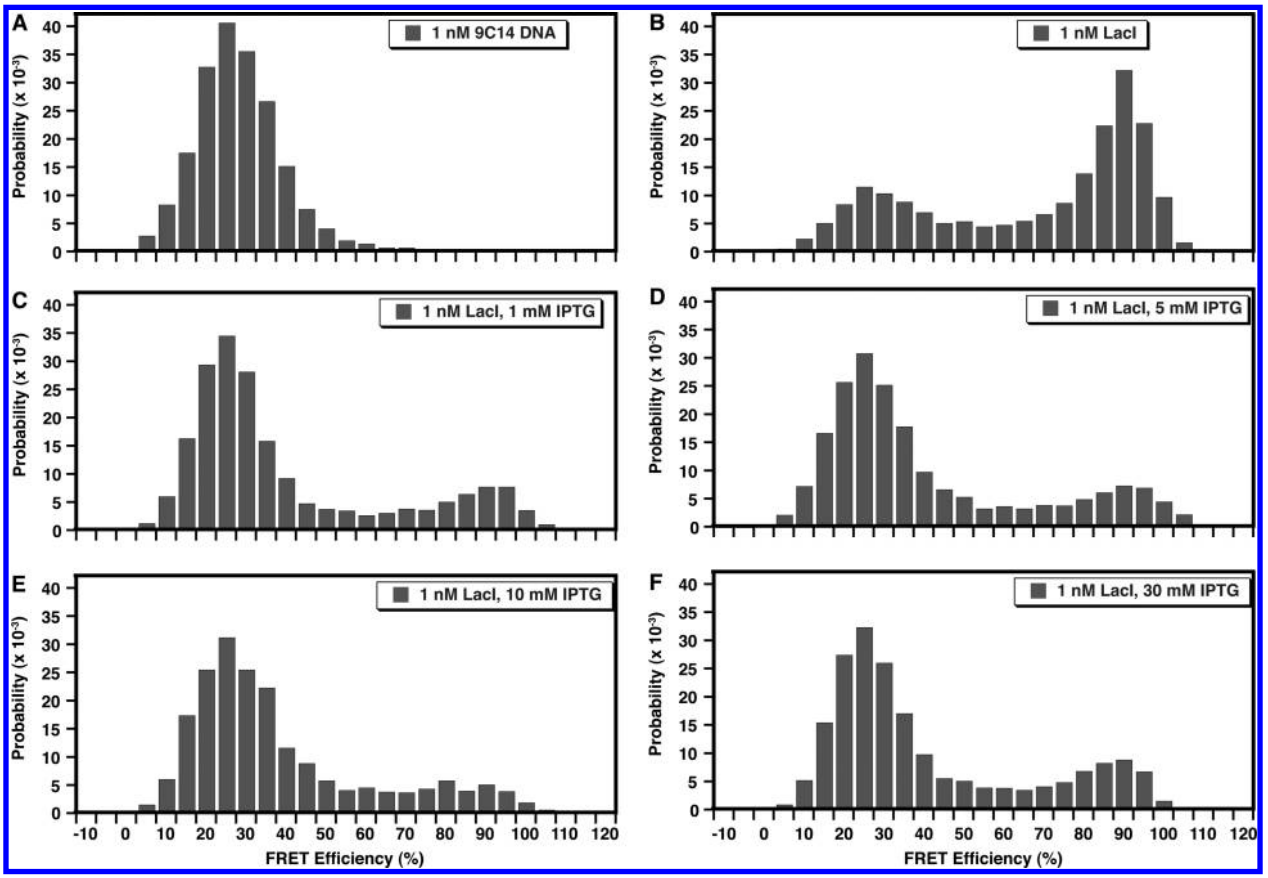

Figure 5. Single-molecule fluorescence experiments on freely diffusing LacI-9C14-IPTG complexes in which LacI was preincubated with IPTG. The experiments were otherwise done as in Figure 4, and the similarity of the results demonstrates that the LacI-DNA-IPTG complexes observed are at equilibrium. (A) FRET histogram of 9C14 DNA alone. (B) LacI-9C14 complexes. (C–F) FRET histograms obtained at 1, 5, 10, and 30 mM IPTG. As in Figure 4, IPTG-bound looped complexes show a persistent high-efficiency peak. The origin of the low-amplitude intermediate apparent FRET efficiencies are discussed in the main text and Supporting Information.

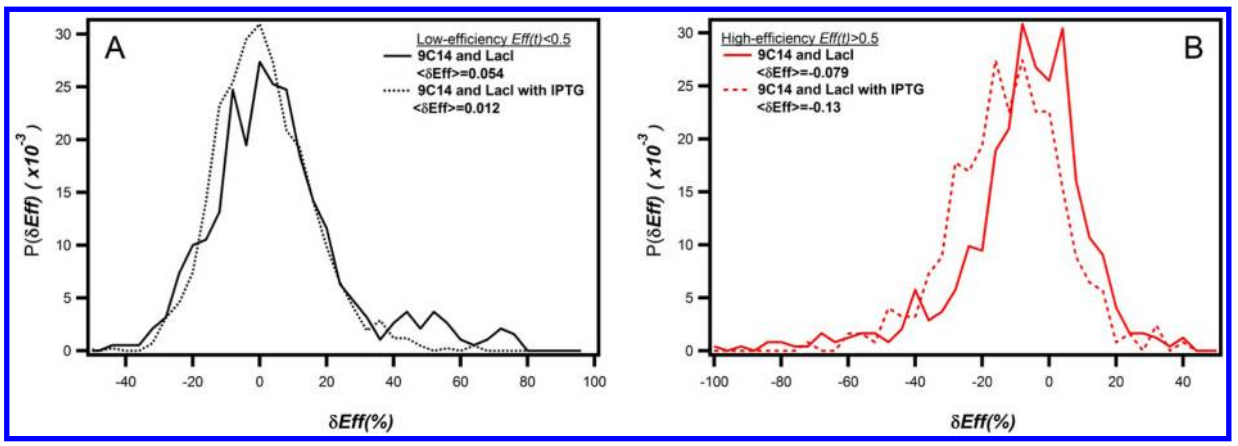

Figure 6. Fluctuation distribution histograms of δEff for the low-efficiency FRET (A) and high-efficiency FRET (B) populations in the presence and absence of IPTG. Details of conditions and calculations are given in the text.

$$[Open] \rightleftarrows [Closed]$$

in which the two states, open and closed, each represent a collection of possible loop geometries. Transitions from low-FRET-efficiency "open" geometries to high-efficiency "closed" geometries are apparent as small peaks with large positive δEff originating from low-efficiency states in Figure 6A. Similarly, negative δEff originating from high-efficiency states in Figure 6B represents closed to open transitions. The values of $[Open]$ and $[Closed]$ were determined by integrating the FRET efficiency histograms over ranges below and above $Eff = 0.5$, respectively, and the closed loop population changed from 31 to 14% upon the addition of IPTG. An increase in the probability of conversion from closed to open forms and a decrease in the open to closed probability are observed when IPTG is added. To address these observations more quantitatively, we can multiply the population fraction for a given state by the probability of exiting that state. At equilibrium the two products should be equal:

dx.doi.org/10.1021/jp308930c | J. Phys. Chem. B XXXX, XXX, XXX–XXX

$$[Open]P_{close} = [Closed]P_{open} \quad (3)$$

The values of P_{close} and P_{open} were estimated by assuming that the negative portion of Figure 6A and the positive portion of Figure 6B are due to statistical fluctuations from photon-counting and loop motions Subtracting these statistical fluctuations from the distributions in Figure 6 gives the probability of fluctuations in the tails of the distribution which are used as estimates for P_{close} and P_{open}:

$$P_{close} = 1 - 2\sum_{i\leq 0} P(\delta Eff)_i$$
$$P_{open} = 1 - 2\sum_{i\geq 0} P(\delta Eff)_i \quad (4)$$

where the indices are the values from the abscissae in Figure 6 from which the respective $P(\delta Eff)$ values were taken. This analysis assumes that in the absence of loop opening and closing, the fluctuation distribution would be symmetric. This approximation holds well for 9C14 in the absence of LacI, where P_{close} = 0.045. Using this approach, the values in Table 1

Table 1. Equilibrium Fluctuation Analysis Results[a]

	9C14+LacI	9C14+LacI+IPTG
$[Open]$ $(E < 0.5)$	0.69	0.86
$[Closed]$ $(E > 0.5)$	0.31	0.14
P_{close}	0.15	0.11
P_{open}	0.30	0.58
$[Open] \times P_{close}$	0.10	0.094
$[Closed] \times P_{open}$	0.093	0.082

[a] E = FRET efficiency. $[Open]$ and $[Closed]$ are the fraction of the total population in each loop state. P_{close} and P_{open} are the probabilities that a transition will convert from open to closed or closed to open, respectively.

were obtained. In the presence of IPTG P_{open} increases, as does the total probability $(P_{open} + P_{close})$ of transitions that switch from one looped state to another, consistent with a model in which interconversion increases in the presence of the inducer. Considering the assumptions, limitations in temporal and spectral resolution of the measurements, and the inability of FRET to accurately report populations in complex systems, the values shown in Table 1 have remarkable consistency with the two-state model of open and closed loops.

Evaluating the first moment of the distributions $<\delta Eff>$ for low- and high-efficiency states in the presence and absence of IPTG confirms that IPTG increases the rate of interconversion and the preference for closed to open transitions: In Figure 6A, $<\delta Eff>$ originating from low-efficiency states decreases from 0.054 in the absence of IPTG to 0.012 at 5 mM. In Figure 6B, this effect is reversed for the closed-loop geometries: the first moment is −0.079 in the absence of IPTG and −0.13 in its presence due to an increased probability for the large decreases in transfer efficiency that accompany the conversion of closed loops to open loops.

The fluctuation analysis proves to be a useful method for evaluating population interconversion for the LacI-DNA system. As stated previously, the error analysis given in the Supporting Information based on standard error propagation techniques shows that the FRET histogram widths and intermediate values observed in Figures 4 and 5 are not sufficient to support an argument for conformational switching between looped populations. Evaluating fluctuations for large and statistically rare events facilitated by 100 μs time resolution provides a method for evaluating loop conformational interchange and not merely photophysical artifacts.

In summary, bulk and single-molecule FRET measurements suggest that LacI-9C14-IPTG exists as at least two populations. One has a closed-form, high-efficiency FRET loop geometry similar to the uninduced LacI-9C14 loop. The other, which does not support FRET, could include loop states with more open LacI protein (moving the dyes apart), different loop topologies, or specific-nonspecific loops. The fluctuation analysis presented in Table 1 strongly supports the notion that conformational switching dynamics are altered by the addition of IPTG, leading to a diversity of loop shapes but not the breaking of loops.

DISCUSSION

Effector molecules and architectural DNA binding proteins regulate loop shape and stability.[39−41] Here we apply EMSA and SM-FRET to investigate the modulation of LacI-DNA looping by IPTG in vitro, using a previously characterized prebent DNA looping substrate (9C14) that supports hyper-stable loops. Inducer-bound Lac repressor undergoes a conformational change that allosterically shifts the headpiece and core domains of the structure,[3] resulting in dramatically decreased affinity for DNA. Previous in vitro and in vivo evidence does indicate that the IPTG-bound LacI is still capable of forming looped complexes. Here a looped species with the same electrophoretic mobility is observed in the presence and absence of IPTG, presumably corresponding to the closed, parallel form of the LacI-9C14 loop.[31] Consistent with these results, in single-molecule diffusing FRET experiments at saturating IPTG, the position but not the amplitude of a high-efficiency FRET peak is maintained. In both the EMSA and the single-molecule FRET studies the addition of excess LacI to the LacI-9C14-IPTG complexes neither increased nor decreased the looped population, suggesting that the initial LacI-9C14-IPTG complexes that do not show FRET are also stable loops. The high-FRET LacI-9C14-IPTG loop presumably has the same closed geometry as the uninduced loop. The stable loops that do not show FRET could include an open form of the LacI protein, a different DNA loop topology,[20,21,32] or looping between an operator and a nonspecific DNA binding site.

The DNA bending in 9C14 appears to be important to the stability of the induced loop. (TPM shows that IPTG breaks loops that lack DNA bending.[42]) We suggest that the bending mimics the supercoiled DNA environment of an *E. coli* cell, in which the high local concentration of the operators allows the formation of LacI-DNA loops despite saturating [IPTG].[43] DNA supercoiling could stabilize a variety of loop shapes and sizes. For example, LacI binding to plectonemic DNA forms loops with the same V-shaped LacI seen in the high-FRET 9C14 loops but an open form LacI could bridge operators in apical loops.[43] We suggest that all of the looped forms are likely to be linked to at least one operator because they are still observed to repress transcription to some extent. We propose that these inducer-bound LacI-DNA looped complexes may control the kinetics of induction and rerepression of the operon. The single-molecule fluctuation analysis (Figure 6 and Table 1) does indeed show that inducer-bound LacI is responsible for shifting the equilibrium of loop geometries by increasing the probability of an open-loop geometry. The

dx.doi.org/10.1021/jp308930c | J. Phys. Chem. B XXXX, XXX, XXX−XXX

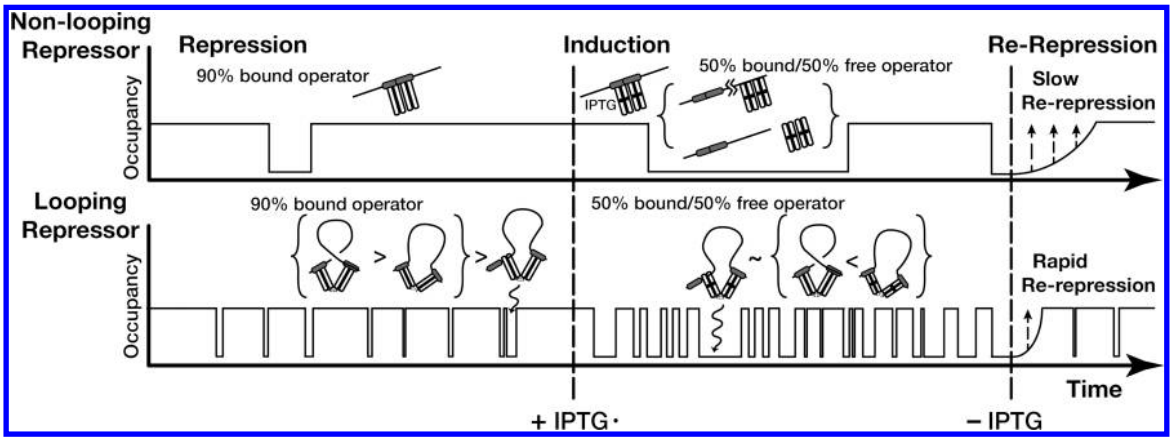

Figure 7. Stochastic model for the functions of alternative DNA loops during repression, induction, and rerepression. Regulation carried out by the Lac repressor, with its proposed ability to form stable specific-nonspecific loops, is compared with regulation by a putative nonlooping protein with the same binding affinity for its (longer) operator site. Equal affinity is indicated in the Figure by equal ratios of on/off times for the two proteins. The on rate for a single-site protein is necessarily slower than that of a looping protein because it cannot locate its operator through direct transfer,[50] and hence the off-rate is also slower at constant affinity. Upon induction, if the nonlooping protein leaves its site, then there is no mechanism for retaining it nearby, whereas a specific-nonspecific loop allows for induction while maintaining nearby LacI. This is most critical to regulatory efficiency when the inducer is removed. The looping protein, being continually localized, can reoccupy its operator very rapidly, whereas the nonlooping protein must diffuse back to the site from elsewhere in the cell. Hence, rerepression is accelerated by the proposed specific−nonspecific looping mechanism, and it also occurs at a more consistent rate.

presence of IPTG also slows the rate of conversion from open to closed but not by a large factor, suggesting that LacI does remain localized near an operator.

Any actual or proposed role for looping should be compared to the regulation that could be carried out by a single-site protein.[44] Looping can confer at least two potential advantages. First, it allows for multiple simultaneous inputs from separate DNA binding sites, which may be essential for regulation of genes with complex responses to the environment, as in development or homeostasis. Furthermore, detailed experiments on the *lac* system suggest that induction increases the apparent torsional rigidity of loop DNA, indicating that the induced loop is more sensitive to poor alignment of operator sites.[7] The control of loop stability by changes in DNA shape and supercoiling is an additional mechanism for modulation of gene regulation.[24,39,45,46]

The other unique function of looping is that local concentration effects confer rapid on/off rates even at high affinity. In contrast, a single-site protein with a larger binding surface would tend to require slow on/off rates for high affinity. Leibler has pointed out that looping is therefore useful to the cell because the low level of transcription initiation that escapes repression occurs at a relatively uniform rate instead of in stochastic bursts.[47] Here we extend this idea to the induced state: loops in which one headpiece of the repressor is bound to nonspecific DNA instead of to the proximal operator would presumably allow induction, but the induced repressor would be retained in the DNA neighborhood through the other headpiece, able to respond rapidly to the disappearance of allolactose.

Figure 7 illustrates this model for the biological consequences of alternative looping. The left half of the Figure illustrates the advantage of fast on/off rates in the repressed state. The right half illustrates that continued localization of the repressor even during induction should accelerate rerepression when the inducer concentration drops. In addition, persistent looping during induction should suppress variability in rates of rerepression that would otherwise be caused by loss of LacI from the local DNA environment. The proposal that induced LacI will remain localized is testable with in vivo single-molecule studies, but existing data do not address it because they have used dimeric repressors.[48] Quantitative models for DNA strain and bending used to explore DNA geometry in gene regulation must be extended to include IPTG-bound loops. Only when this is done will it be possible for systems biology models to fully reflect the relevance of changes in looping cooperativity as well as simple binding affinity.

■ CONCLUSIONS

This work has demonstrated the use of bulk and single-molecule methods to investigate the IPTG-induced changes in LacI-DNA loop geometries. SM-FRET confirmed that the high-FRET LacI-9C14 loop is only partially destabilized by saturating IPTG. LacI titration experiments and FRET fluctuation analysis suggest that the addition of IPTG induces loop conformational dynamics and re-equilibration between loop population distributions that include a mixture of looped states that do not exhibit high-efficiency FRET. The results show that repression by looping even at saturating IPTG should be considered in models for regulation of the operon. We propose that persistent DNA loops near the operator function biologically to accelerate rerepression upon exhaustion of inducer.

■ ASSOCIATED CONTENT

Ⓢ Supporting Information

Descriptions and figures describing the LacI protein characterization and single-molecule FRET error analysis. This information is available free of charge via the Internet at http://pubs.acs.org.

■ AUTHOR INFORMATION

Corresponding Author

*E-mail: doug.english@wichita.edu; jdkahn@umd.edu.

dx.doi.org/10.1021/jp308930c | J. Phys. Chem. B XXXX, XXX, XXX−XXX

Present Address
[§]Department of Biochemistry and Molecular Biology, Johns Hopkins Bloomberg School of Public Health, 615 N. Wolfe St., Baltimore, MD 21205.

Notes
The authors declare no competing financial interest.

■ ACKNOWLEDGMENTS

K.A.G. acknowledges support from the E.I. DuPont Graduate Fellowship Award via NOBCChE and a College of Life Sciences Board of Visitors Fellowship, University of Maryland, College Park. A.R.H. was partially supported by the Dr. Herman Kraybill Fellowship. We are grateful to Dr. Herman Sintim and his lab for fluorimeter access and to Dr. Steven Rokita and his group for access to other shared equipment. Preliminary work was supported by an NSF Career Award to J.D.K. D.S.E. acknowledges support from Wichita State University.

■ REFERENCES

(1) Jacob, F.; Monod, J. *J. Mol. Biol.* **1961**, *3*, 318−356.
(2) Friedman, A. M.; Fischmann, T. O.; Steitz, T. A. *Science* **1995**, *268*, 1721−1727.
(3) Lewis, M.; Chang, G.; Horton, N. C.; Kercher, M. A.; Pace, H. C.; Schumacher, M. A.; Brennan, R. G.; Lu, P. *Science* **1996**, *271*, 1247−1254.
(4) Oehler, S.; Amouyal, M.; Kolkhof, P.; von Wilcken-Bergmann, B.; Müller-Hill, B. *EMBO J.* **1994**, *13*, 3348−3355.
(5) Phillips, R.; Kondev, J.; Theriot, J. *Physical Biology of the Cell*; Garland Science: New York, 2008.
(6) Sanyal, A.; Lajoie, B. R.; Jain, G.; Dekker, J. *Nature* **2012**, *489*, 109−113.
(7) Becker, N. A.; Kahn, J. D.; Maher, L. J., III. *J. Mol. Biol.* **2005**, *349*, 716−730.
(8) O'Gorman, R. B.; Rosenberg, J. M.; Kallai, O. B.; Dickerson, R. E.; Itakura, K.; Riggs, A. D.; Matthews, K. S. *J. Biol. Chem.* **1980**, *255*, 10107−10114.
(9) Donner, J.; Caruthers, M. H.; Gill, S. J. *J. Biol. Chem.* **1982**, *257*, 14826−14829.
(10) Ohshima, Y.; Mizokoshi, T.; Horiuchi, T. *J. Mol. Biol.* **1974**, *89*, 127−136.
(11) Bell, C. E.; Lewis, M. *Nat. Struct. Biol.* **2000**, *7*, 209−214.
(12) Lewis, M. *C. R. Biol.* **2005**, *328*, 521−548.
(13) Kao-Huang, Y.; Revzin, A.; Butler, A. P.; O'Conner, P.; Noble, D. W.; von Hippel, P. H. *Proc. Natl. Acad. Sci. U.S.A.* **1977**, *74*, 4228−4232.
(14) Yagil, G.; Yagil, E. *Biophys. J.* **1971**, *11*, 11−27.
(15) Boezi, J. A.; Cowie, D. B. *Biophys. J.* **1961**, *1*, 639−647.
(16) Oehler, S.; Alberti, S.; Müller-Hill, B. *Nucleic Acids Res.* **2006**, *34*, 606−612.
(17) Mossing, M. C.; Record, M. T. *Science* **1986**, *233*, 889−892.
(18) Bell, C. E.; Barry, J.; Matthews, K. S.; Lewis, M. *J. Mol. Biol.* **2001**, *313*, 99−109.
(19) Daber, R.; Sharp, K.; Lewis, M. *J. Mol. Biol.* **2009**, *392*, 1133−1144.
(20) Semsey, S.; Virnik, K.; Adhya, S. *Trends Biochem. Sci.* **2005**, *30*, 334−341.
(21) Lillian, T. D.; Goyal, S.; Kahn, J. D.; Meyhöfer, E.; Perkins, N. C. *Biophys. J.* **2008**, *95*, 5832−5842.
(22) Kahn, J. D.; Cheong, R.; Mehta, R. A.; Edelman, L. M.; Morgan, M. A. *Biophys. Rev. Lett.* **2006**, *1*, 327−341.
(23) Kramer, H.; Amouyal, M.; Nordheim, A.; Müller-Hill, B. *EMBO J.* **1988**, *7*, 547−556.
(24) Whitson, P. A.; Hsieh, W. T.; Wells, R. D.; Matthews, K. S. *J. Biol. Chem.* **1987**, *262*, 14592−14599.
(25) McKay, D. B.; Pickover, C. A.; Steitz, T. A. *J. Mol. Biol.* **1982**, *156*, 175−183.
(26) Ruben, G. C.; Roos, T. B. *Microsc. Res. Technol.* **1997**, *36*, 400−416.
(27) Wong, O. K.; Guthold, M.; Erie, D. A.; Gelles, J. *PLoS Biol.* **2008**, *6*, e232.
(28) Mehta, R. A.; Kahn, J. D. *J. Mol. Biol.* **1999**, *294*, 67−77.
(29) Crothers, D. M.; Haran, T. E.; Nadeau, J. G. *J. Biol. Chem.* **1990**, *265*, 7093−7096.
(30) Edelman, L. M.; Cheong, R.; Kahn, J. D. *Biophys. J.* **2003**, *84*, 1131−1145.
(31) Morgan, M. A.; Okamoto, K.; Kahn, J. D.; English, D. S. *Biophys. J.* **2005**, *89*, 2588−2596.
(32) Haeusler, A. R.; Goodson, K. A.; Lillian, T. D.; Wang, X.; Goyal, S.; Perkins, N. C.; Kahn, J. D. *Nucleic Acids Res.* **2012**, *40*, 4432−4445.
(33) Brenowitz, M.; Mandal, N.; Pickar, A.; Jamison, E.; Adhya, S. *J. Biol. Chem.* **1991**, *266*, 1281−1288.
(34) Wilson, C. J.; Zhan, H.; Swint-Kruse, L.; Matthews, K. S. *Biophys. Chem.* **2007**, *126*, 94−105.
(35) Deniz, A. A.; Laurence, T. A.; Dahan, M.; Chemla, D. S.; Schultz, P. G.; Weiss, S. *Annu. Rev. Phys. Chem.* **2001**, *52*, 233−253.
(36) Schuler, B.; Lipman, E. A.; Eaton, W. A. *Nature* **2002**, *419*, 743−747.
(37) Dahan, M.; Deniz, A. A.; Ha, T.; Chemla, D. S.; Schulz, P. G.; Weiss, S. *Chem. Phys.* **2001**, *247*, 85−106.
(38) Bates, M.; Blosser, T. R.; Zhuang, X. *Phys. Rev. Lett.* **2005**, *94*, 108101.
(39) Lobell, R. B.; Schleif, R. F. *J. Mol. Biol.* **1991**, *218*, 45−54.
(40) Dalma-Weiszhausz, D. D.; Brenowitz, M. *Biochemistry* **1992**, *31*, 6980−6989.
(41) Hoover, T. R.; Santero, E.; Porter, S.; Kustu, S. *Cell* **1990**, *63*, 11−22.
(42) Finzi, L.; Gelles, J. *Science* **1995**, *267*, 378−380.
(43) Maher, L. J.; Bond, L. M.; Peters, J. P.; Becker, N. A.; Kahn, J. D. *Nucleic Acids Res.* **2010**, *38*, 8072−8082.
(44) Schleif, R. *Nature* **1987**, *327*, 369−370.
(45) Carmona, M.; Magasanik, B. *J. Mol. Biol.* **1996**, *261*, 348−356.
(46) Lobell, R. B.; Schleif, R. F. *Science* **1990**, *250*, 528−532.
(47) Vilar, J. M.; Leibler, S. *J. Mol. Biol.* **2003**, *331*, 981−989.
(48) Elf, J.; Li, G. W.; Xie, X. S. *Science* **2007**, *316*, 1191−1194.
(49) Koo, H. S.; Drak, J.; Rice, J. A.; Crothers, D. M. *Biochemistry* **1990**, *29*, 4227−4234.
(50) von Hippel, P. H.; Berg, O. G. *J. Biol. Chem.* **1989**, *264*, 675−678.